Neurotransmitter contribution of neuronal subpopulations affect properties of the circadian clock

Chen, X.Y.; Gu, C.G.; Zheng, W.X.; Yang, H.J.; Rohling, J.H.T.

Nonlinear Dyn (2024) 112:17433–17443
https://doi.org/10.1007/s11071-024-09914-z

ORIGINAL PAPER

Neurotransmitter contribution of neuronal subpopulations affect properties of the circadian clock

Xuanyu Chen · Changgui Gu · Wenxin Zheng · Huijie Yang · Jos H. T. Rohling

Received: 27 December 2023 / Accepted: 18 June 2024 / Published online: 27 June 2024

Abstract In mammals, the suprachiasmatic nucleus (SCN) orchestrates the circadian rhythms even without the daily light–dark cycle (resulting in free running behavior). The SCN neurons can be organized into two heterogeneous subgroups, namely the ventrolateral (VL) subgroup and the dorsomedial (DM) subgroup, which are coupled through different neurotransmitters, i.e., the VL and the DM produce VIP and AVP, respectively. Experiments have found that they also differ in their neural amplitudes. In the present study, we examined the effect of disparities in transmitter signals released by two subgroups on the collective behaviors of the SCN neurons, in particular the free running period and the synchronization degree. The disparity of transmitter signals released by the VL and the DM is represented by the ratio of weight parameters in the mean-field, based on the Poincaré model. We find that the effects depend on the difference of neuronal amplitudes between the two subgroups. If there exists an amplitude difference between the subpopulations, the relationship of the free running period to the ratio is parabolic with a trough. Additionally, the relation between the synchronization degree and the coupling strength is also dependent on the ratio of weight parameters in the mean-field. Interestingly, when the ratio is large, the synchronization degree shows a parabolic-like change with the increase of the coupling strength. Our findings shed light on the rhythmic regulations of the SCN neurons affected by the disparities in the strengths of transmitters released by different subpopulations.

Keywords Circadian rhythms · SCN neuronal network · Mean-field · Free running period

1 Introduction

In mammals, including humans, the suprachiasmatic nucleus (SCN) serves as an endogenous clock regulating a 24-h rhythm in behavioral and physiological activities, adjusting it to the external light–dark cycle [1–3]. Dysregulation of the circadian clock can lead to health problems such as insomnia and metabolic disorders [4,5], but is even a risk factor for neurodegenerative diseases and cancer [6,7]. A good mechanistic understanding of the SCN is crucial to reduce negative effects of rhythmic disorders and achieve better therapeutic effects for diseases [8,9].

Located in the hypothalamus above the optic chiasm, the SCN is comprised of about 20,000 neurons [10]. Been observed in cell culture of the rat SCN, the

Supplementary Information The online version contains supplementary material available at https://doi.org/10.1007/s11071-024-09914-z.

X. Chen · C. Gu (✉) · W. Zheng · H. Yang
Department of Systems Science, Business School, University of Shanghai for Science and Technology, Shanghai 200093, China
e-mail: Gu_changgui@163.com

J. H. T. Rohling
Department of Cell and Chemical Biology, Leiden University Medical Center, 2300RC Leiden, The Netherlands

isolated individual neuron is capable of producing circadian oscillations with intrinsic periods ranging from 20 to 28 h [11,12]. The nonidentical neurons are coupled through neurotransmitters to form a SCN network in which a uniform period for the neuronal ensemble emerges [13,14]. The neuronal ensemble in the SCN is able to produce an endogenous rhythm that is close to 24 h, without the influence of the timing cues of the external light–dark conditions. Here the coupling between the neurons plays a key role in the function of the SCN to produce such an endogenous rhythm of approximately 24 h [15–18]. The endogenous period that is produced can be seen in the activity-rest period of the mammals that are placed in constant dark conditions, and is called the free running period (FRP). The FRP differs among species. For instance, the FRP is close to 24.4 h in Drosophila, close to 25.6 h in Zebrafish, about 28 h in Phaseolus, it varies from 23.5 to 24.5 h for Bat, from 23.5 to 24 h for Squirrel, and from 24.2 h to 25.1 h for people, where it should be noted that humans are usually not recorded in constant darkness but in constant dim light conditions [15,19–21].

The SCN neurons are organized in multiple subpopulations of neurons, depending on neurotransmitter content and function. Anatomically, the two most important subpopulations can be found in the Ventrolateral part (VL) and Dorsomedial part (DM) of the SCN. With respect to the distinct function, the VL neurons are sensitive to the input light information via the retinohypothalamic tract (RHT) [22], whereas the DM neurons receive the light information from the VL region [23,24]. Therefore, the VL neurons are primarily responsible for adjusting the 24-h rhythm to a new timezone after a transatlantic flight, as these neurons resynchronize to the shifted light–dark cycle far more rapidly than the DM neurons [25,26]. Being involved in the communication between the neurons in the SCN, different substances that act as neurotransmitters are released by the VL and the DM. In the VL part, vasoactive intestinal polypeptide (VIP) is produced, while arginine vasopressin (AVP) is produced in the DM part. Gamma-aminobutyric acid (GABA) is released in both regions of the SCN [10,26–28]. VIP is considered to mediate the synchronization between the neurons to photic cues, while AVP is rhythmically regulated by the clock [29–31]. On the other hand, the broadly expressed AVP signals have been found to coordinate circadian oscillations in the absence of VIP [32]. Although the interaction between the neurons within the SCN is mainly achieved by these neurotransmitters [33,34], the exact mechanisms of coupling is still not understood.

Next to synchronization between the neurons and neuronal subpopulations, neural amplitudes are also important for proper clock function. The amplitude of the rhythmic SCN ensemble output is of utmost importance to impose a healthy rhythm on the rest of the body. A reduction in rhythmic amplitude can lead to the deterioration of rhythm, causing sleep problems and even disease [35]. It is suggested that the lower amplitudes of the SCN neuronal activities from aged animals are related to the decline in their overt rhythms [36,37]. Not much is known about the amplitude in the different subregions of the SCN. A previous study has reported that the amplitudes of the clock gene expression of Period2 in the VL part is smaller than that in the DM part [38]. Others addressed that the amplitude was independent of which part the SCN neuron belonged to [39,40]. Moreover, a damped oscillator (zero intrinsic amplitude) driven by noise can act similar to a self-sustained oscillator so that it becomes difficult to determine whether an oscillator is self-sustained or damped [41].

In the SCN network, each neuron has an impact on the other neurons in the network by producing the neurotransmitters mentioned before [42]. In addition, each neuron is under influence of the other neurons in the network by its absorbing capacity of neurotransmitters. The absorbing capacity (which we shall call coupling strength) modifies circadian properties of the neuron, such as amplitude and phase of operation [43–45]. For simplicity, we will use the frequently used mean-field coupling paradigm. Each neuron releases transmitters and thus contributes to the mean-field by its weight parameter, and is influenced by the mean-field through its coupling strength. The different subpopulations of neurons show differences in their contribution weights and coupling strengths. For example, the VL neurons produce VIP which is received by the DM neurons. It has been found that the dispersion in the coupling affects the length of the endogenous period of the SCN, and through this the FRP. Typically, the FRP decreases with the increase of the dispersion of coupling strength [17]. More recently, it has been found that the dispersion of coupling strengths increases the FRP in the presence of a negative relationship between the coupling strength and natural period for each neuron [18].

However, it remains unclear whether the disparities of strengths of transmitters released by the nonidentical SCN subpopulations affect the FRP.

In the current study, a modified Poincaré model is proposed to examine the effect of disparities of weight parameters in the mean-field on the FRP. Specially, the SCN neurons are coupled through the mean-field of the transmitters, thus they can be regarded as a fully connected network. For simplicity, we assume that the absorbing ability is identical but the contribution differs for the SCN neurons. In Sec. 2, the Poincaré model is introduced to describe the nonidentical neuronal oscillators of the SCN. Simulation results are shown about the relationship of the FRP and the synchronization to the dispersion in Sec. 3. Theoretical analyses are given to confirm the simulation results in Sec. 4. The conclusions and discussions are presented in Sec. 5.

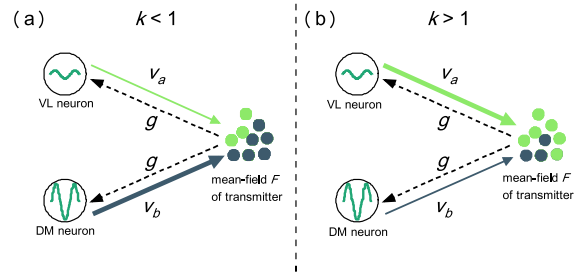

Fig. 1 Scheme of the heterogeneity on neuronal amplitudes and strength of transmitters released by two subgroups. In the mean-field F, v_a (or v_b) determines the strength of transmitters released by the VL (or the DM) neuron, k represents the ratio of weight parameter v_a to v_b, with **a** $k < 1$ and **b** $k > 1$. The thickness of the solid arrow represents the magnitude of v. The light (or dark) green solid circle represents transmitter released by the VL (or the DM) neuron. The amplitude of curve in the empty circle represents the intrinsic amplitude. The dashed arrow represents the identical sensibility, i.e., the coupling strength g of the individual neuron to F

2 Description of model

Several models have been introduced to describe the circadian oscillators, including the Goodwin model and the Poincaré model [46,47]. In the Goodwin model, the rhythmic expression of core clock gene is simulated by a transcriptional feedback loop [43,45], while in the Poincaré model, the rhythmicity of the clock gene is abstracted by the amplitude-phase oscillation (r, θ) that transforms intuitively from the polar coordinates to the Cartesian coordinates (x, y) [48].

In this article, we select the Poincaré model as it provides a more straightforward way for theoretical analysis. The evolution equations of N neuronal oscillators can be written as [3,18,49–53],

$$\begin{aligned} \dot{x_i} &= \gamma x_i\,(a_i - r_i) - \omega_i y_i + gF, \\ \dot{y_i} &= \gamma y_i\,(a_i - r_i) + \omega_i x_i, i = 1, 2, ..., N, \end{aligned} \tag{1}$$

where x_i and y_i represent the temporal horizontal and vertical coordinate values for the ith oscillator. ω_i and a_i are the natural frequency and intrinsic amplitude of oscillator i, characterizing the period and amplitude of rhythmic clock gene expression of a single cell. γ is the relaxation parameter representing the rigidity to the external amplitude disturbance. r_i stands for the coupled amplitude with $r_i = \sqrt{x_i^2 + y_i^2}$. For $i = 1, ..., N_1$, oscillator i belongs to the VL population, while for $i = N_1 + 1, ..., N$, oscillator i belongs to the DM population. The oscillators are coupled through the mean-field term gF, where F denotes the mean-field of transmitters released by the SCN neurons and g is the global coupling strength representing the sensitivity to F. F is given by:

$$F = \frac{1}{N}\sum_{i=1}^{N} v_i x_i, \tag{2}$$

where $\frac{1}{N}\sum_{i=1}^{N} v_i = 1$. v_i is the contribution weight for oscillator i in the mean-field, which denotes the strength of transmitters released by oscillator i. v_i differs between neuronal types since the VL and DM oscillators release VIP and AVP respectively. For simplicity, we set the values of v_i to be the same within the VL or the DM, but differ between the two subgroups. Therefore, the weight parameters are $v_i = v_a$ for $i = 1, ..., N_1$ and $v_i = v_b$ for $i = N_1 + 1, ..., N$ in the mean-field. In the present study, we assume that $N_1 = \frac{N}{2}$, and define $k = \frac{v_a}{v_b}$ as the ratio for measuring the disparities of v_i between the VL and the DM. Correspondingly, when $v_b \neq 0$, we obtain $v_a = \frac{2k}{k+1}$ and $v_b = \frac{2}{k+1}$, $k \in (0, \infty)$. If $k = 1$, the values of v_i are equal between the VL neurons and the DM neurons, i.e., no disparity. If $k \neq 1$, the disparity emerges as indicated in Fig. 1.

To characterize the difference in intrinsic amplitudes between the VL and the DM subpopulations, we set $a_i = A_1$ for $i = 1, ..., N_1$ and $a_i = A_2$ for $i = N_1 + 1, ..., N$. $\bar{A} = \frac{A_1 + A_2}{2}$ is the mean intrinsic amplitude and $\delta = \frac{A_2 - A_1}{2}$ denotes the difference of intrinsic amplitudes between the VL and the DM

neurons. It can be seen that $\delta = A_2 - \bar{A} = \bar{A} - A_1$. Because the results are symmetric for positive and negative values of δ, we set $\delta \geqslant 0$. If $\delta = 0$ the amplitudes of two populations are equivalent, and if $\delta > 0$ the VL oscillators rotate with lower amplitudes. However, we can generalize this for lower amplitude oscillatory rhythms in the DM. Note that throughout the article, the heterogeneity between the VL and the DM lies in the difference of the intrinsic amplitudes as well as ratio k of the weight parameters in the mean-field, as depicted in Fig. 1. The natural frequency of oscillators ω_i in the SCN neurons satisfies a normal distribution $N\left(\bar{\omega}, \sigma^2\right)$, where $\sigma = 0.005$. In numerical simulations, other parameter values are employed as Ref. [3], i.e., $\gamma = 1h^{-1}$, $\bar{A} = 1$, and $\bar{\omega} = \frac{2\pi}{24}h^{-1}$.

The collective rhythm of the population is measured by the macroscopic order parameter,

$$R = \left\langle \left| \frac{1}{N} \sum_{j=1}^{N} e^{i\theta_j} \right| \right\rangle, \tag{3}$$

where $\langle \cdot \rangle$ denotes the time average, $\theta_j = \arctan \frac{y_j}{x_j}$ represents the phase of oscillator j. $R \in [0, 1]$, in which $R = 0$ describes the incoherence among all oscillators (no synchronization) and $R = 1$ describes the stable synchronous state for whole population (perfect synchronization). In order to monitor the changes in synchronization between the VL and the DM subregions, the inter-group synchronization degree R_{VD} is calculated by:

$$R_{VD} = \frac{1}{N_1(N - N_1)} \sum_{j=1}^{N_1} \sum_{l=1+N_1}^{N} R_{jl}, \tag{4}$$

where $R_{jl} = \left\langle \left| \frac{1}{2}(e^{i\theta_j} + e^{i\theta_l}) \right| \right\rangle$ denotes the phase synchronization between oscillator j and oscillator l. Therefore, R_{VD} is attained by averaging the degrees of synchronization between all pairs of oscillators between the VL and the DM.

3 Simulation results

The numerical simulations of the model were performed with a network size of $N = 200$ neuronal oscillators. Since the fourth-order Runge–Kutta method provides higher accuracy than the Euler method, it was adopted for numerical simulations with time increments of 0.01 h. The initial 2, 000, 000 time steps (20, 000 h) were neglected as to avoid the effect of transients. Initial values for variables x_i and y_i were selected randomly from a uniform distribution between 0 and 1.

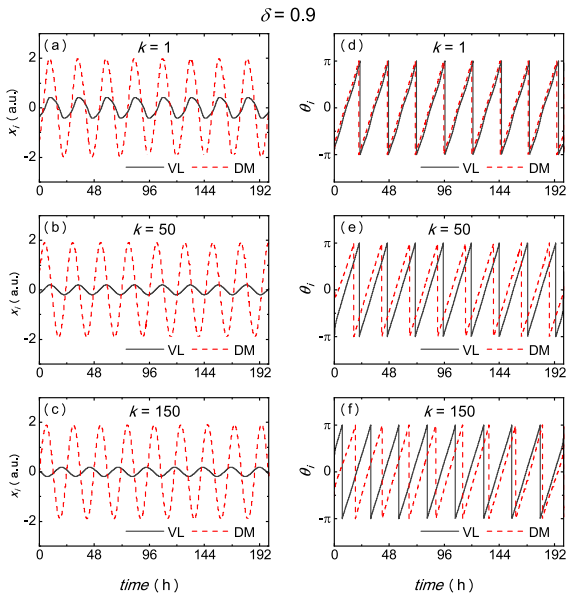

Fig. 2 Temporal evolution of two oscillators from the VL and the DM with selected value of k, respectively, marked by the variable x_i in (**a**–**c**) and the phase θ_i in (**d**–**f**). The difference of the intrinsic amplitude is $\delta = 0.9$, and the coupling strength is $g = 0.15$. Note that in the Poincaré model, the unit of x_i is expressed by a.u. since it is an abstracted variable

Figure 2 illustratively displays the temporal evolution of the oscillators affected by the ratio k, including the evolution for the oscillating variables x (a-c) and for the phases θ (d-f). Larger values of k indicate that the VL neurons have larger weight parameters in the mean-field, which means that the strength of transmitters released by the VL is larger. In Fig. 2a and d, it is easy to see that when no dispersion emerges in the weight parameters, the whole network is uniformly coupled and perfectly synchronized. In Fig. 2b and e, when the weight v_a of the VL neurons is 50 times larger than v_b of the DM neurons, the neurons are well synchronized but the phase difference between two subgroups emerges. In (c) and (f), when the ratio k increases to 150, the DM neurons are running out of synchronization with the VL neurons because the period of both populations differs. Thus, the noteworthy change of synchronization between two subgroups is attributed to the disparities of v.

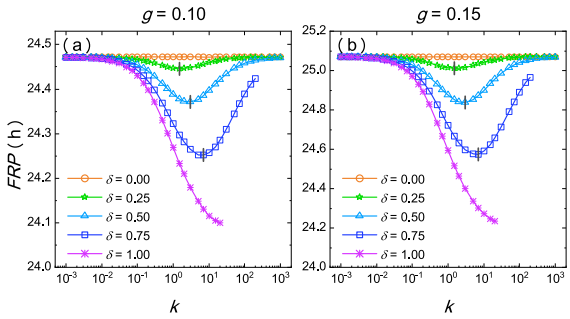

Fig. 3 The relationship of the FRP to the key parameter k. The coupling strengths are set to be $g = 0.10$ in (**a**), and $g = 0.15$ in (**b**). The deviation for the distribution of the nature frequency is $\sigma = 0.005$, and δ is the difference in the intrinsic amplitudes. The vertical line (grey) marks off the valley value of the FRP under numerical simulation. Note that for $\delta = 0.75$ and 1.00, some values of the FRP are not available because the neurons start to lose synchronization, which causes the FRP rhythm generated by the SCN network to become instable

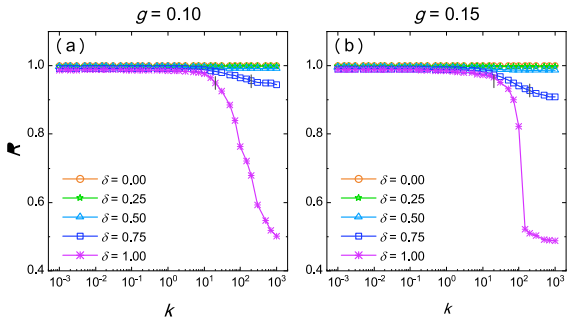

Fig. 4 The relationship of the synchronization degree R to the key parameter k. The coupling strengths are set to **a** $g = 0.10$, and **b** $g = 0.15$. Other parameters are adopted as the same in Fig. 3. Note that the vertical line (grey) marks off the k value at which the FRP becomes instable (see Fig. 3) because the periods of some neurons start to become inconsistent and different from the periods of other neurons, thus the uniform rhythm of the whole SCN is lost

In Fig. 3, we examine the relationship of the FRP to the ratio k. The FRP is the free-running period of the animal that is dictated by the neuronal activity of the SCN as a whole, which again depends strongly on the synchronization of the neurons in the SCN. Only if the neurons are well synchronized, the SCN is able to produce a rhythm and cause the animal to free-run (have a FRP). It is visible that the results are affected by the difference δ in intrinsic amplitudes. If there are no difference in intrinsic amplitudes, the value of the FRP is independent of k, which turns out to be a constant around 24.46 h in (a) and 25.07 h in (b). If the difference δ in amplitudes is not zero between VL and DM, we see that the free running period (FRP) is not constant any longer for all ratios k between the transmission weights of both subgroups. A parabolic change in FRP with a trough emerges when k becomes larger. If the amplitude difference δ becomes larger, the trough value of the FRP becomes increasingly smaller. These troughs occur at different values for k. The trough of the FRP is around $k = 1.5$, 3 and 7 for the following values of $\delta = 0.25$, 0.50 and 0.75, respectively. If the difference $\delta = 1.00$, i.e., the VL oscillators are damped, the FRP decreases continuously as k increases until the running periods of some neurons become inconsistent. Then the synchronization between neurons becomes lost and the SCN rhythm is lost. In this case, at around $k = 22$ the periods of the individual neurons start to become dispersed, resulting in the unavailability of the FRP.

To examine quantitatively how the disparities in strength of transmitters released by both subgroups affect the synchronization of the SCN, Fig. 4 shows the relationship of the synchronization degree R to the ratio k. R plays a key role for the rhythm robustness in the SCN. In the panel (a) or (b), the synchronization degree R holds a constant value 1 if $\delta = 0$, i.e., there are no amplitude difference between two subgroups. In this case, the ratio of weight parameters in the mean-field does not influence the synchronization degree. If the difference δ emerges in intrinsic amplitudes, the synchronization degree R starts to decline with the increase of k. Moreover, the degree R decreases more rapidly for larger values of δ. This means that if the amplitude difference δ is larger, the synchronization between the neurons decreases more rapidly when the ratio between the transmission weights increases, i.e., when the weights of one subgroup (VL) becomes larger than the other subgroup (DM). Comparing (a) and (b), an interesting result is observed from $\delta = 0.75$, i.e., the decline in synchronization degree R is actually less for the smaller value of coupling strength g. The results indicate that for larger values of k, a worse synchronous state emerges when the coupling strength g is larger.

In order to explore the interesting results shown in Fig. 4 in detail, we examine the relationship of the synchronization degree R to coupling strength g with selected values of the ratio k and amplitude difference δ in Fig. 5. If there are no difference in amplitudes, R increases monotonically with the increase of g when g is small, and roughly becomes a constant when g is large. If the difference δ emerges in intrinsic ampli-

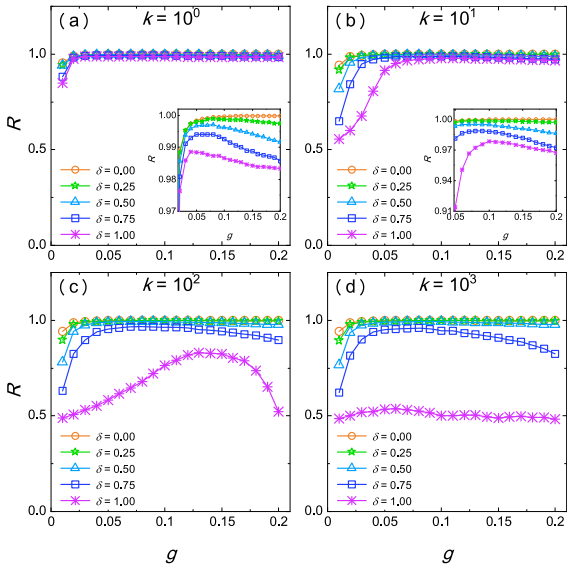

Fig. 5 The effect of the ratio k on the relationship of the synchronization degree R to the coupling strength g. The insets of **a** and **b** are zooms of R around 1. Other parameters are adopted as the same in Fig. 4

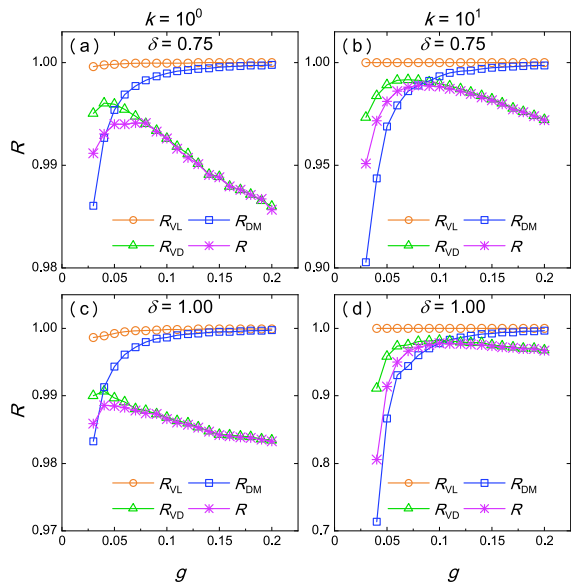

Fig. 6 The relationship of respective synchronization degrees R, R_{VL}, R_{DM} and R_{VD} to the coupling strength g. The ratio is set to $k = 1$ in (**a**) and (**c**), $k = 10$ in (**b**) and (**d**). The difference of intrinsic amplitudes is set to $\delta = 0.75$ in (**a**) and (**b**), $\delta = 1.00$ in (**c**) and (**d**). R accounts for the global synchronization degree, R_{VL} (or R_{DM}) represents the synchronization degree of the VL (or the DM) neurons, and R_{VD} characterizes that between the VL and the DM neurons

tudes, the relationship of R to g is parabolic with a peak value. As seen in panel (a) or (b), when the weight parameter of the VL is the same as or about 10 times larger than that of the DM, R first increases with the increase of g and then slightly decreases with g exceeding a certain value g_c. Typically, g_c is around 0.08 if the amplitude difference $\delta = 0.25, 0.50$ and 0.75. If the amplitude difference $\delta = 1.00$, g_c is approximately 0.04 in (a) and 0.10 in (b). With extreme large k values, i.e., the DM neurons release very few transmitters, it can be found that the relationship of R to g is similarly parabolic in (c) or (d). Note that when the ratio $k = 10^3$, the value of R fluctuates around 0.5 if the VL oscillators are damped (Fig. 5d). In this case, no significant change occurs in the synchronization degree with the increase of g.

Additionally, we examine whether the parabolic changes of R in Fig. 5 derive from the synchronization degree of oscillators within the group or the synchronization degree between groups, namely R_{VL}, R_{DM} and R_{VD} (Fig. 6). We select the case in which $\delta = 0.75$ or 1.00 to be a clear example. The ratio is set to $k = 1$ and 10, i.e., there is no heterogeneity in the strengths of transmitters released by two subgroups or the strength of transmitters released by the VL neuron is larger than that of the DM neuron. In (a-d), it is visible that the synchronization degree R_{VL} is around 1 within the VL subgroup where the neurons have smaller intrinsic amplitudes. On the other hand, the synchronization degree R_{DM} within the DM subgroup, in which the neurons have larger intrinsic amplitudes, increases with the rising coupling strength g when g is a small term, and approximates to 1 when g is large. Furthermore, in (a-d) the synchronization degree R_{VD} displays parabolic changes and approaches to the values of R with the increase of g. For a focused value of g, the value of R_{VD} is visibly smaller than 1. Therefore, when the strength of transmitter signals released by the VL subgroup is larger than that of the DM subgroup, the global synchronization is improved by the enhancement of R_{DM} and R_{VD}, while for larger values of g, it is weakened mainly due to the decrease of R_{VD} between two subgroups.

4 Analytical results

For simplicity of theoretical analysis, Eq. (1) can be transformed to polar coordinates by $x_i = r_i \cos\theta_i$ and

$y_i = r_i \sin\theta_i$. Taken $\gamma = 1$ into account, the dynamics of the amplitude r and the phase δ for oscillator i take the form:

$$\begin{aligned} \dot{r}_i &= r_i\,(a_i - r_i) + \frac{g}{N}\sum_{j=1}^{N} v_j r_j \cos\theta_j \cos\theta_i, \\ \dot{\theta}_i &= \omega_i - \frac{g}{r_i N}\sum_{j=1}^{N} v_j r_j \sin\theta_j \sin\theta_i, \end{aligned} \tag{5}$$

for $i = 1, ..., N$. According to the definition of the mean-field F, a new parameter is introduced as

$$F_r e^{i\phi} = \frac{1}{N}\sum_{j=1}^{N} v_j r_j e^{i\theta_j}, \tag{6}$$

where $\theta_j(t)$ and $r_j(t)$ are the phase and the amplitude of oscillator j, $\phi(t)$ and $F_r(t)$ are the phase and the amplitude of the mean-field, respectively. Considering the definitions provided by Eq. (6), we obtain

$$F_r \cos\phi = \frac{1}{N}\sum_{j=1}^{N} v_j r_j \cos\theta_j, \tag{7}$$

the dynamical equations, Eq. (5) can be reduced to

$$\begin{aligned} \dot{r}_i &= r_i\,(a_i - r_i) + g F_r \cos(\theta_i - \phi), \\ \dot{\theta}_i &= \omega_i - \frac{g F_r}{r_i}\sin(\theta_i - \phi), \end{aligned} \tag{8}$$

where $(\theta_i - \phi)$ is the phase difference between the individual oscillator i and the mean-field. As illustrated in Fig. 7, the values of $\sin(\theta_i - \phi)$ split into two clusters if $\delta > 0$, which correspond to the VL neuron oscillators and the DM neuron oscillators, respectively.

In the following, we set a reference rotating frame, $\psi(t) = \psi(0) + \Omega t$, being Ω the mean frequency. Imposing that all oscillators are frequency locked, $\dot{\phi} = \Omega$ can be derived. For the simplicity of the analysis, we set $\phi - \Omega t \equiv 0$. Through the transformation $\vartheta_i = \theta_i - \Omega t$, Eq. (8) becomes:

$$\begin{aligned} \dot{r}_i &= r_i\,(a_i - r_i) + g F_r \cos\vartheta_i, \\ \dot{\vartheta}_i &= (\omega_i - \Omega) - \frac{g F_r}{r_i}\sin\vartheta_i, \end{aligned} \tag{9}$$

in which ϑ_i denotes the phase difference between oscillator i and the mean-field. On the condition that $\sin\vartheta_i \in [-1, 1]$, $|\omega_i - \Omega| \le \frac{g F_r}{r_i}$, $\dot{r}_i = 0$ and $\dot{\vartheta}_i = 0$ are obtained for stationary solutions. Based on the first equation of Eq. (9),

$$\cos\vartheta_i = \frac{r_i\,(r_i - a_i)}{g F_r}. \tag{10}$$

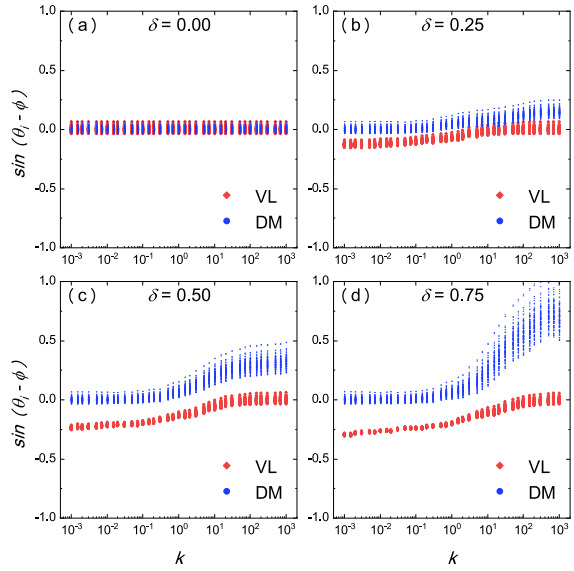

Fig. 7 The evolutionary of $\sin(\theta_i - \phi)$ versus the ratio k for the chosen values of δ. The Red (or blue) dot accounts for the sine value of the phase difference between the VL oscillators (or the DM oscillators) and the mean-field. The coupling strength is $g = 0.15$

To move one step further, some mild approximations are assumed, $r_1 \approx ... \approx r_{N_1} = r_a$ and $r_{N_1+1} \approx ... \approx r_N = r_b$, where r_a and r_b refer to the mean coupled amplitude for the VL and the DM, respectively. According to Eq. (10), the values of $\cos\vartheta_i$ can be approximated to an average $\cos\vartheta_a$ for the VL oscillators and $\cos\vartheta_b$ for the DM oscillators. From Eq. (7), the general expression of F_r is simplified as

$$\begin{aligned} F_r &= \frac{1}{N}\left[\sum_{j=1}^{N_1} v_i r_i \cos\vartheta_i + \sum_{j=N_1+1}^{N} v_i r_i \cos\vartheta_i\right] \\ &\approx \frac{k}{k+1} r_a \cos\vartheta_a + \frac{1}{k+1} r_b \cos\vartheta_b. \end{aligned} \tag{11}$$

Substituting Eq. (10) into Eq. (11) yields

$$F_r \approx \sqrt{\frac{k r_a^2 (r_a - A_1) + r_b^2 (r_b - A_2)}{g(k+1)}}. \tag{12}$$

It is found in Eq. (12) that for $k \ll 1$, $\frac{k r_a^2 (r_a - A_1)}{g(k+1)}$ is a very small term, thus the value of F_r depends mainly on the ratio k and the mean amplitude r_b of the DM subgroup. For $k \gg 1$, $\frac{r_b^2 (r_b - A_2)}{g(k+1)}$ is a very small term, thus the value of F_r depends mainly on the ratio k and the mean amplitude r_a of the VL subgroup.

Back to the dynamic of the population, given by Eq. (9), the average coupling frequency can be

expressed as

$$\Omega = \bar{\omega_i} - \frac{gkF_r}{(k+1)r_a}\sin\vartheta_a - \frac{gF_r}{(k+1)r_b}\sin\vartheta_b, \quad (13)$$

In the case of $\delta = 0$, two subgroups show no heterogeneity in neither coupled amplitudes nor phases, thus $\sin\vartheta_a$ and $\sin\vartheta_b$ are around 0, while $\cos\vartheta_a$ and $\cos\vartheta_b$ are around 1. From Eq. (9), the solutions for amplitudes and frequency are

$$\begin{aligned} r_a &= r_b = \bar{A} + g, \\ \Omega &= \bar{\omega_i}. \end{aligned} \quad (14)$$

Consequently, the effective frequency Ω remains unchanged along with the variation of k. On the other hand, for $\delta > 0$, we consider the cases in which $k \ll 1$, $k \approx 1$ and $k \gg 1$.

When $k \ll 1$, Eq. (12) is altered to be

$$F_r \approx r_b\sqrt{\frac{r_b - A_2}{g(k+1)}}. \quad (15)$$

The phase difference between the VL oscillator (or the DM oscillator) and the mean-field is a small term at $k \ll 1$, therefore $\cos\vartheta_a \approx 1$ and $\cos\vartheta_b \approx 1$. By substituting Eq. (15) into Eq. (10), the solutions for the amplitudes are

$$\begin{aligned} r_a &\approx \frac{A_1 + \sqrt{A_1^2 + \frac{4gr_b}{k+1}}}{2}, \\ r_b &\approx A_2 + \frac{g}{k+1}, \end{aligned} \quad (16)$$

where $A_1 = \bar{A} - \bar{A}\delta$, $A_2 = \bar{A} + \bar{A}\delta$. Note that the negative solution for R_1 is discarded. An example in Fig. 8 illustrates the comparison between the numerical simulations and the theoretical results of average coupled amplitudes at $k = 0.01$.

As shown in Fig. 7, $\sin\vartheta_a < 0$ and $\sin\vartheta_b \approx 0$ can be obtained when $k \ll 1$. Substituting Eq. (16) into Eq. (15),

$$F_r \approx \frac{r_b}{k+1}. \quad (17)$$

Thus Eq. (13) is rewritten as

$$\Omega \approx \bar{\omega_i} - \frac{gkr_b}{(k+1)^2 r_a}\sin\vartheta_a. \quad (18)$$

Since $\frac{k}{(k+1)^2}$ increases constantly at $k \ll 1$, Ω increases gradually due to the rising k, which leads to the reduction of the FRP. Moreover, the larger frequency Ω emerfges at larger values of $\frac{r_b}{r_a}$, which results from the larger

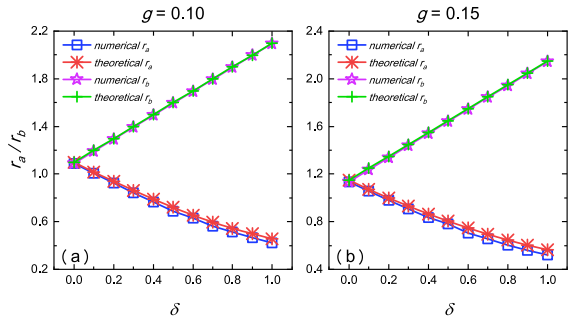

Fig. 8 The comparison between numerical simulations and theoretical results of average coupled amplitudes r_a for the VL and r_b for the DM when $k = 0.01$. The intrinsic amplitude dispersion δ is set from 0.0 to 1.0 with $\Delta\delta = 0.1$. The coupling strength is $g = 0.10$ in (**a**) and $g = 0.15$ in (b)

difference in intrinsic amplitudes between two subgroups.

For the case $k \approx 1$, we consider the ratio to be $k = 1 + \epsilon$, in which $\epsilon > 0$ represents a small positive number. Therefore Eq. (13) becomes

$$\Omega = \bar{\omega_i} - gF_r\left[\frac{1+\epsilon}{(2+\epsilon)r_a}\sin\vartheta_a + \frac{1}{(2+\epsilon)r_b}\sin\vartheta_b\right]. \quad (19)$$

As shown in Fig. 7, we have $\sin\vartheta_a < 0$, $\sin\vartheta_b > 0$ and $|\sin\vartheta_a| > |\sin\vartheta_b|$ for $k = 1 + \epsilon$. Based on Eq. (19), $\frac{1+\epsilon}{(2+\epsilon)r_a}$ increases and $\frac{1}{(2+\epsilon)r_b}$ decreases with the increase of ϵ. Therefore, the frequency Ω continues to increase with the increase of ϵ, which leads to the decrease of the FRP.

When $k \gg 1$, Eq. (12) can be approximated by

$$F_r \approx r_a\sqrt{\frac{k(r_a - A_1)}{g(k+1)}}. \quad (20)$$

Thus when the oscillators are fully synchronous, by substituting Eq. (20) into Eq. (13), we have

$$\Omega \approx \bar{\omega_i} - \sqrt{g\,(r_a - A_1)}\left(\frac{k}{k+1}\right)^{\frac{3}{2}}\sin\vartheta_a. \quad (21)$$

Since $\sin\vartheta_a \to 0$ with $k \to \infty$ (see Fig. 7), the frequency Ω decreases and approximates to $\bar{\omega_i}$ until the oscillators are out of synchronization. As a result, a valley value of the free running period occurs at $k > 1$, which fits the numerical simulations shown in Fig. 3.

5 Conclusion and discussion

The circadian properties of the SCN are affected by the inter-cellular coupling through neurotransmitters,

such as VIP produced by the VL and AVP produced by the DM [27,28]. In this article, we examine whether the disparities in strength of transmitters released by the VL and the DM neurons affect the free running period (FRP), which is a measure for the period of the rhythm. Based on the Poincaré model, we characterize the disparity as the ratio of weight parameters in the mean-field between two subgroups. It is found that the effects depend on the difference in intrinsic amplitudes between the VL and the DM. In detail, the relationship between the FRP and the ratio is parabolic with a trough if a moderate difference in amplitude is present. Furthermore, the disparities appear to be crucial for the global synchronization of the neurons in the SCN. The synchronization degree of the SCN neurons are important for the rhythm robustness. For the SCN to be responsive to external changes, the neurons are only loosely synchronized [13,54–56]. Our analysis shows that this can only be accomplished if the VL neurons have a lower amplitude rhythm but a larger weight parameter than the DM neurons. Moreover, this global synchronization also depends on the global coupling strength of the neurons, which shows a parabolic-like change with a maximum at a certain global coupling strength value.

To evaluate our method, the effect of disparities in transmitter signals released by two subgroups is also examined using the Goodwin model, with the limitation of ratio k from 10^{-1} to 10^{1} (see the Supplementary Material). It turns out that the numerical results are qualitatively consistent with those based on the Poincaré model. In the Goodwin model, differences in coupled amplitudes are much smaller between two subgroups, which can already lead to changes in the rhythmic behaviors of the SCN neurons, namely the FRP and the synchronization.

The disparities in strengths of transmitters released by the VL and the DM subgroups have been studied in previous works [42,57]. An experimental study has reported that the FRP is lengthened when AVP released by the dorsal part of the SCN reduces, which also causes the heterogeneity in the contributions [58]. On the other hand, our results suggest that if the disparities between the VL and the DM are larger, the FRP is larger. Therefore, the heterogeneity may partially contribute to the variation found between species. Although not much is known about amplitude differences in the different regions of the SCN, it is unlikely that the actual amplitude differences are substantial. In Ref. [38], the amplitude of rhythms in the dispersed VL part of the rat SCN is nearly half of that of the DM part. If the difference in amplitudes is small, it implies that the FRP and the synchronization changes slightly with the ratio of disparities. For this the interaction of transmitters and the contribution of GABA are needed to understand the generation of such disparities in the releasing strengths of transmitters [59–61].

The Poincaré model is a general model that studies the circadian oscillations without quantitatively considering the biochemical process of neuronal transcription or firing. Therefore, it is often applied to explain the relative differences such as phases, periods and connections between the SCN neurons. Our findings show an inspiration for future experiments and studies on the rhythmic regulation of different transmitters released by the SCN subpopulations.

Funding This work is supported by the National Natural Science Foundation of China under Grant Nos. 12275179 and 11875042, Natural Science Foundation of Shanghai (Grant No. 21ZR1443900).

Data availibility The authors declare that the manuscript has no associated data.

Declarations

Conflict of interest The authors declare that they have no Conflict of interest.

References

1. Pittendrigh, C.S.: Temporal organization: reflections of a Darwinian clock-watcher. Annu. Rev. Physiol. **55**(1), 17–54 (1993)
2. Refinetti, R.: Circadian Physiology. CRC Press, Boca Raton (2006)
3. Abraham, U., Granada, A.E., Westermark, P.O., Heine, M., Kramer, A., Herzel, H.: Coupling governs entrainment range of circadian clocks. Mol. Syst. Biol. **6**(1), 426–438 (2010)
4. Srinivasan, V., Singh, J., Pandi-Perumal, S.R., Brown, G.M., Spence, D.W., Cardinali, D.P.: Jet lag, circadian rhythm sleep disturbances, and depression: the role of melatonin and its analogs. Adv. Ther. **27**(11), 796–813 (2010)
5. Sato, S., Solanas, G., Peixoto, F.O., Bee, L., Symeonidi, A., Schmidt, M.S., Brenner, C., Masri, S., Benitah, S.A., Sassone-Corsi, P.: Circadian reprogramming in the liver identifies metabolic pathways of aging. Cell **170**(4), 664–677 (2017)
6. Masri, S., Sassone-Corsi, P.: The emerging link between cancer, metabolism, and circadian rhythms. Nat. Med. **24**(12), 1795–1803 (2018)

7. Leng, Y., Musiek, E.S., Hu, K., Cappuccio, F.P., Yaffe, K.: Association between circadian rhythms and neurodegenerative diseases. Lancet Neurol. **18**(3), 307–318 (2019)
8. Roenneberg, T., Merrow, M.: The circadian clock and human health. Curr. Biol. **26**(10), R432–R443 (2016)
9. Kelleher, F.C., Rao, A., Maguire, A.: Circadian molecular clocks and cancer. Cancer Lett. **342**(1), 9–18 (2014)
10. Yamaguchi, S., Isejima, H., Matsuo, T., Okura, R., Yagita, K., Kobayashi, M., Okamura, H.: Synchronization of cellular clocks in the suprachiasmatic nucleus. Science **302**(5649), 1408–1412 (2003)
11. Welsh, D.K., Logothetis, D.E., Meister, M., Reppert, S.M.: Individual neurons dissociated from rat suprachiasmatic nucleus express independently phased circadian firing rhythms. Neuron **14**(4), 697–706 (1995)
12. Honma, S., Nakamura, W., Shirakawa, T., Honma, K.: Diversity in the circadian periods of single neurons of the rat suprachiasmatic nucleus depends on nuclear structure and intrinsic period. Neurosci. Lett. **358**(3), 173–176 (2004)
13. Herzog, E.D., Aton, S.J., Numano, R., Sakaki, Y., Tei, H.: Temporal precision in the mammalian circadian system: a reliable clock from less reliable neurons. J. Biol. Rhythms **19**(1), 35–46 (2004)
14. Rohling, J.H.T., Vanderleest, H.T., Michel, S., Vansteensel, M.J., Meijer, J.H.: Phase resetting of the mammalian circadian clock relies on a rapid shift of a small population of pacemaker neurons. PLoS ONE **6**(9), e25437 (2011)
15. Czeisler, C.A., Duffy, J.F., Shanahan, T.L., Brown, E.N., Mitchell, J.F., Rimmer, D.W., Ronda, J.M., Silva, E.J., Allan, J.S., Emens, J.S., et al.: Stability, precision, and near-24-hour period of the human circadian pacemaker. Science **284**(5423), 2177–2181 (1999)
16. Daido, H.: Why circadian rhythms are circadian: competitive population dynamics of biological oscillators. Phys. Rev. Lett. **87**(4), 048101 (2001)
17. Gu, C., Wang, J., Liu, Z.: Free-running period of neurons in the suprachiasmatic nucleus: its dependence on the distribution of neuronal coupling strengths. Phys. Rev. E **80**(3 Pt 1), 030904 (2009)
18. Gu, C., Rohling, J.H.T., Liang, X., Yang, H.: Impact of dispersed coupling strength on the free running periods of circadian rhythms. Phys. Rev. E **93**(3), 032414 (2016)
19. Ahlgren, A., Halberg, F.: Cycles of Nature: An Introduction to Biological Rhythms. National Science Teachers Association, Washington, D.C. (1990)
20. Kurosawa, G., Goldbeter, A.: Amplitude of circadian oscillations entrained by 24-h light-dark cycles. J. Theor. Biol. **242**(2), 478–488 (2006)
21. Middleton, B., Arendt, J., Stone, B.: Human circadian rhythms in constant dim light (8 lux) with knowledge of clock time. J. Sleep Res. **5**(2), 69–76 (1996)
22. Colwell, C.S.: Linking neural activity and molecular oscillations in the SCN. Nat. Rev. Neurosci. **12**(10), 553–569 (2011)
23. Lee, H.S., Nelms, J.L., Nguyen, M., Silver, R., Lehman, M.N.: The eye is necessary for a circadian rhythm in the suprachiasmatic nucleus. Nat. Neurosci. **6**(2), 111–112 (2003)
24. Moore, R.Y., Speh, J.C., Leak, R.K.: Suprachiasmatic nucleus organization. Cell Tissue Res. **309**(1), 89–98 (2002)
25. Nagano, M., Adachi, A., Nakahama, K., Nakamura, T., Tamada, M., Meyer-Bernstein, E., Sehgal, A., Shigeyoshi, Y.: An abrupt shift in the day/night cycle causes desynchrony in the mammalian circadian center. J. Neurosci. **23**(14), 6141–6151 (2003)
26. Albus, H., Vansteensel, M.J., Michel, S., Block, G.D., Meijer, J.H.: A GABAergic mechanism is necessary for coupling dissociable ventral and dorsal regional oscillators within the circadian clock. Curr. Biol. **15**(10), 886–893 (2005)
27. Aton, S.J., Colwell, C.S., Harmar, A.J., Waschek, J., Herzog, E.D.: Vasoactive intestinal polypeptide mediates circadian rhythmicity and synchrony in mammalian clock neurons. Nat. Neurosci. **8**(4), 476–483 (2005)
28. Morin, L.P.: SCN organization reconsidered. J. Biol. Rhythms **22**(1), 3–13 (2007)
29. Reed, H.E., Meyer-Spasche, A., Cutler, D.J., Coen, C.W., Piggins, H.D.: Vasoactive intestinal polypeptide (VIP) phase-shifts the rat suprachiasmatic nucleus clock in vitro. Eur. J. Neurosci. **13**(4), 839–843 (2001)
30. Harmar, A.J., Marston, H.M., Shen, S., Spratt, C., West, K.M., Sheward, W.J., Morrison, C.F., Dorin, J.R., Piggins, H.D., Reubi, J., et al.: The $VPAC_2$ receptor is essential for circadian function in the mouse suprachiasmatic nuclei. Cell **109**(4), 497–508 (2002)
31. Herzog, E.D., Hermanstyne, T., Smyllie, N.J., Hastings, M.H.: Regulating the suprachiasmatic nucleus (SCN) circadian clockwork: interplay between cell-autonomous and circuit-level mechanisms. Cold Spring Harb. Perspect. Biol. **9**(1), a027706 (2017)
32. Maywood, E.S., Chesham, J.E., O'Brien, J.A., Hastings, M.H.: A diversity of paracrine signals sustains molecular circadian cycling in suprachiasmatic nucleus circuits. Proc. Natl. Acad. Sci. U.S.A. **108**(34), 14306–14311 (2011)
33. Shirakawa, T., Honma, S., Honma, K.: Multiple oscillators in the suprachiasmatic nucleus. Chronobiol. Int. **18**(3), 371–387 (2001)
34. Hastings, M.H., Herzog, E.D.: Clock genes, oscillators, and cellular networks in the suprachiasmatic nuclei. J. Biol. Rhythms **19**(5), 400–413 (2004)
35. Meijer, J.H., Colwell, C.S., Rohling, J.H.T., Houben, T., Michel, S.: Dynamic neuronal network organization of the circadian clock and possible deterioration in disease. Prog. Brain Res. **199**, 143–162 (2012)
36. Aujard, F., Herzog, E.D., Block, G.D.: Circadian rhythms in firing rate of individual suprachiasmatic nucleus neurons from adult and middle-aged mice. Neuroscience **106**(2), 255–261 (2001)
37. Yamazaki, S., Straume, M., Tei, H., Sakaki, Y., Menaker, M., Block, G.D.: Effects of aging on central and peripheral mammalian clocks. Proc. Natl. Acad. Sci. U.S.A. **99**(16), 10801–10806 (2002)
38. Evans, J.A., Suen, T., Callif, B.L., Mitchell, A.S., Castanon-Cervantes, O., Baker, K.M., Kloehn, I., Baba, K., Teubner, B.J.W., Ehlen, J.C.: Shell neurons of the master circadian clock coordinate the phase of tissue clocks throughout the brain and body. BMC Biol. **13**, 1 (2015)
39. Webb, A.B., Angelo, N., Huettner, J.E., Herzog, E.D.: Intrinsic, nondeterministic circadian rhythm generation in identified mammalian neurons. Proc. Natl. Acad. Sci. U.S.A. **106**(38), 16493–16498 (2009)

40. Webb, A.B., Taylor, S.R., Thoroughman, K.A., Doyle, F.J., Herzog, E.D.: Weakly circadian cells improve resynchrony. PLoS Comput. Biol. **8**(11), e1002787 (2012)
41. Westermark, P.O., Welsh, D.K., Okamura, H., Herzel, H.: Quantification of circadian rhythms in single cells. PLoS Comput. Biol. **5**(11), e1000580 (2009)
42. Shan, Y., Abel, J.H., Li, Y., Izumo, M., Cox, K.H., Jeong, B., Yoo, S., Olson, D.P., Doyle, F.J., Takahashi, J.S.: Dual-color single-cell imaging of the suprachiasmatic nucleus reveals a circadian role in network synchrony. Neuron **108**(1), 164–179 (2020)
43. Gonze, D., Bernard, S., Waltermann, C., Kramer, A., Herzel, H.: Spontaneous synchronization of coupled circadian oscillators. Biophys. J . **89**(1), 120–129 (2005)
44. Bernard, S., Gonze, D., Čajavec, B., Herzel, H., Kramer, A.: Synchronization-induced rhythmicity of circadian oscillators in the suprachiasmatic nucleus. PLoS Comput. Biol. **3**(4), e68 (2007)
45. Locke, J.C., Westermark, P.O., Kramer, A., Herzel, H.: Global parameter search reveals design principles of the mammalian circadian clock. BMC Syst. Biol. **2**, 1–9 (2008)
46. Bodenstein, C., Gosak, M., Schuster, S., Marhl, M., Perc, M.: Modeling the seasonal adaptation of circadian clocks by changes in the network structure of the suprachiasmatic nucleus. PLoS Comput. Biol. **8**(9), e1002697 (2012)
47. Schmal, C., Myung, J., Herzel, H., Bordyugov, G.: A theoretical study on seasonality. Front. Neurol. **6**, 94 (2015)
48. Tokuda, I.T., Ono, D., Ananthasubramaniam, B., Honma, S., Honma, K., Herzel, H.: Coupling controls the synchrony of clock cells in development and knockouts. Biophys. J . **109**(10), 2159–2170 (2015)
49. Gu, C., Ramkisoensing, A., Liu, Z., Meijer, J.H., Rohling, J.H.T.: The proportion of light-responsive neurons determines the limit cycle properties of the suprachiasmatic nucleus. J. Biol. Rhythms **29**(1), 16–27 (2014)
50. Gu, C., Tang, M., Rohling, J.H.T., Yang, H.: The effects of non-self-sustained oscillators on the en-trainment ability of the suprachiasmatic nucleus. Sci. Rep. **6**(1), 37661 (2016)
51. Bordyugov, G., Abraham, U., Granada, A., Rose, P., Imkeller, K., Kramer, A., Herzel, H.: Tuning the phase of circadian entrainment. J. R. Soc. Interface **12**(108), 20150282 (2015)
52. Gu, C., Xu, J., Liu, Z., Rohling, J.H.T.: Entrainment range of nonidentical circadian oscillators by a light-dark cycle. Phys. Rev. E **88**(2), 022702 (2013)
53. Gu, C., Yang, H., Ruan, Z.: Entrainment range of the suprachiasmatic nucleus affected by the difference in the neuronal amplitudes between the light-sensitive and light-insensitive regions. Phys. Rev. E **95**(4), 042409 (2017)
54. Ono, D., Weaver, D.R., Hastings, M.H., Honma, K., Honma, S., Silver, R.: The suprachiasmatic nucleus at 50: looking back, then looking forward. J. Biol. Rhythms **39**(2), 135–165 (2024)
55. Liu, A.C., Welsh, D.K., Ko, C.H., Tran, H.G., Zhang, E.E., Priest, A.A., Buhr, E.D., Singer, O., Meeker, K., Verma, I.M., et al.: Intercellular coupling confers robustness against mutations in the SCN circadian clock network. Cell **129**(3), 605–616 (2007)
56. Michel, S., Meijer, J.H.: From clock to functional pacemaker. Eur. J. Neurosci. **51**(1), 482–493 (2020)
57. Tokuda, I.T., Ono, D., Honma, S., Honma, K., Herzel, H.: Coherency of circadian rhythms in the SCN is governed by the interplay of two coupling factors. PLoS Comput. Biol. **14**(12), e1006607 (2018)
58. Mieda, M., Ono, D., Hasegawa, E., Okamoto, H., Honma, K., Honma, S., Sakurai, T.: Cellular clocks in AVP neurons of the SCN are critical for interneuronal coupling regulating circadian behavior rhythm. Neuron **85**(5), 1103–1116 (2015)
59. Hastings, M.H., Maywood, E.S., Brancaccio, M.: Generation of circadian rhythms in the suprachiasmatic nucleus. Nat. Rev. Neurosci. **19**(8), 453–469 (2018)
60. Honma, S.: The mammalian circadian system: a hierarchical multi-oscillator structure for generating circadian rhythm. J. Physiol. Sci. **68**(3), 207–219 (2018)
61. DeWoskin, D., Myung, J., Belle, M.D.C., Piggins, H.D., Takumi, T., Forger, D.B.: Distinct roles for GABA across multiple timescales in mammalian circadian timekeeping. Proc. Natl. Acad. Sci. U.S.A. **112**(29), E3911–E3919 (2015)